Composites Part B 90 (2016) 232–240

Contents lists available at ScienceDirect

Composites Part B

journal homepage: www.elsevier.com/locate/compositesb

Dowelled structural connections in laminated bamboo and timber

Thomas Reynolds [a, *], Bhavna Sharma [c], Kent Harries [b], Michael Ramage [a]

[a] Natural Materials and Structures Research Group, Department of Architecture, University of Cambridge, United Kingdom
[b] Department of Civil and Environmental Engineering, University of Pittsburgh, United States
[c] BRE Centre for Innovative Construction Materials, Department of Architecture and Civil Engineering, University of Bath, United Kingdom

ARTICLE INFO

Article history:
Received 5 August 2015
Received in revised form
13 November 2015
Accepted 28 November 2015
Available online 7 January 2016

Keywords:
Bamboo
B. Fracture
B. Stress concentrations
C. Analytical modelling
D. Mechanical testing

ABSTRACT

Structural sections of laminated bamboo can be connected using methods common in timber engineering, however the different material properties of timber and laminated bamboo suggest that the behaviour of connections in the two materials would not be the same. This study investigates the dowelled connection, in which a connector is passed through a hole in the material, and load is resisted by shear in the connector and embedment into the surrounding material. Steel dowels were used in a connection between a laminated bamboo member and a steel plate in a central slot in the bamboo, and the behaviour of this connection was compared with a similar connection in timber. The laminated bamboo was made from Moso bamboo (*Phyllostachys pubescens*) which had been treated by one of two preservative processes, either bleaching or caramelisation. Following testing, substantial qualitative differences between the bamboo and timber specimens were observed: the bamboo failed most often by the formation of a shear plug whereas the timber failed by a single split. The two preservative treatments resulted in different behaviour: the bleached bamboo had a degree of ductility roughly twice that of the caramelised bamboo. Digital image correlation provided full-field strain measurements, which gave further insight into the differences between the materials, particularly between bamboo and timber. Shear strain is dominant in the bamboo, compared with tensile strain perpendicular to grain in the timber. Numerical modelling showed that this difference in the strain field could be explained by the different orthotropic elastic and frictional properties of the two materials.

1. Introduction

The embedment behaviour of laminated bamboo loaded by a steel bar through a drilled hole was studied. This form of connection is widely used in timber construction, and is known as a dowelled connection. For timber, plastic theory by Johansen [1] allows prediction of the load-carrying capacity of these types of connections, and forms the basis of design standards such as Eurocode 5 [2]. Since laminated bamboo has not been widely used for structural framing, the behaviour of this type of connection in bamboo has yet to be fully characterised.

In Johansen's method, the behaviour of both materials is modelled as being rigid before yield, and perfectly plastic thereafter. Therefore, the diameter and yield strength of the steel dowel are required, in order to calculate the work done in the plastic hinges formed in the dowel at failure. The other parameter required is the embedment strength of the timber around the dowel. This is not a fundamental mechanical property, but a function of fundamental properties used as a measure of how a dowelled system behaves under load. No reliable method exists to calculate this directly from the mechanical properties of the timber. Empirical rules provide a correlation between embedment strength and density. The rules in Eurocode 5 Ref. [2] relate embedment strength to density based on a series of tests carried out by Whale et al. [3].

Other research has sought to investigate the stress distribution and fracture properties that lead to failure of the timber in embedment. Full-field strain measurement by digital image correlation [4,5] and grey-field photoelasticity [6] has provided insight into the deformation of the timber around the connector. This work has shown that orthotropic elastic models of the timber can replicate the measured strains, as long as the frictional contact between connector and timber can be adjusted to match the measurements. This frictional behaviour is very difficult to predict *a priori*, and studies have shown its importance to the embedment strength and stress distribution, in experiments using dowels with high- or low-friction surfaces [5,7].

* Corresponding author.
E-mail address: tpsr2@cam.ac.uk (T. Reynolds).

http://dx.doi.org/10.1016/j.compositesb.2015.11.045

This form of connection is not limited to natural orthotropic materials, and has been widely studied in manufactured fibre-reinforced composites. As manufactured materials, their behaviour may be more accurately predicted based on the known mechanical properties of the materials forming the composite. As a result, finite element models generally show good correlation to experimental results, for prediction of stress distribution [8] and failure modes [9]. Failure criteria have been developed for fibre-reinforced composites, which allow for failure by matrix cracking, fibre-matrix shearing and fibre breakage [10]. A similar approach to describing failure mechanisms should be possible in bamboo.

In timber, the ultimate failure of the connection is generally by a crack originating near the centre of the loaded edge of the hole, in mixed-mode shear and tension [11]. Before the ultimate failure, a yield point is apparent [12]. In timber, this yield point, associated with local bearing failure, is not well defined and requires standard rules to determine its value from force–displacement curves [13].

Fracture in timber connections generally occurs as a single crack initiated from the edge of the hole, progressing in the grain direction, a process referred to as splitting. The fracture toughness K_{IC} measured for such a crack ranges between approximately 200 and 500 kPa $m^{1/2}$ for softwoods [14,15]. The fracture toughness of full-culm bamboo for a crack progressing parallel to the longitudinal axis of the culm is slightly lower, ranging from 150 to 200 kPa $m^{1/2}$ [16]. In both timber and bamboo, the fracture toughness is an order of magnitude or more higher perpendicular to the grain [14,17]. Both timber and bamboo are formed from many long cells, and crack propagation through the material follows a path around the cells through the lignin matrix [18]. These similarities in microscale properties suggest that if the distribution of stress in the material is the same, the cracks formed in bamboo and timber may be similar. Yet our observations suggest otherwise.

The distribution of stress and strain in the material resulting from the force applied by the connector is dependent on the orthotropic properties of the material. The bamboo species used in this study is Moso (*Phyllostachys pubesecens*). The comparison of the properties of Moso bamboo with Sitka spruce in Table 1 shows higher axial strength in the bamboo, but similar axial stiffness in the grain direction, for example. These differences may be expected to lead to different distributions of stress and strain in the material around the connector, affecting the response of the connection to load.

2. Objectives

The present work aims to characterise the performance of dowelled connections in engineered Moso bamboo. The experimental results are compared to timber to ascertain the differences in material embedment and fracture behaviour. Numerical modelling of the strain around the connector is presented for further comparison and compared with full-field strain measurements made during tests.

3. Experimental program materials and methods

To compare both embedment and fracture behaviours in the materials tested, specimens were loaded using a steel dowel in the arrangement most prone to splitting: a loaded edge in the grain direction, as shown Test A in Fig. 1.

The test procedure followed EN 383 [19], the European norm for embedment testing of timber, with an adjustment to allow full-field strain measurement. The surface of the specimens needed to be exposed to allow digital image correlation (DIC) to be used for strain measurement, so a central steel plate was used to apply the load. The materials were loaded using a 12 mm diameter steel dowel passing through a 6.35 mm thick steel plate located in an 8 mm wide central slot machined into each specimen. A tensile load was applied to the specimen, and resisted by embedment of the dowel into the timber or bamboo. The specimens were clamped top and bottom in hydraulic wedge grips. The displacement of the steel plate was measured relative to the edge of the specimen using a single clip gauge to measure the relative displacement of two brackets, one fixed to the specimen, and one to the steel plate, as shown in Fig. 2. The clip gauge effectively measures the average relative displacement at the outer edges of each specimen. The total loaded thickness of the material was 30 mm, or 2.5 times the diameter of the dowel, complying with the requirement of EN 383 [19].

This study used a commercially available laminated bamboo board made from Moso bamboo and a soy-based resin (Smith & Fong Plyboo). The specimens were built up from 19 mm thick laminated bamboo sheet (2440 × 1220 × 19 mm), cut and further laminated into sections of the required dimensions using polyurethane adhesive (Purbond HB S309). The adhesive was applied manually with a glue proportion of 180 g/m^2 (final product). The laminas were pressed using manual clamps to apply a pressure of 0.6 MPa for 4 h. The laminas were orientated so that the radial direction in the culm from which they were cut was in the plane of the specimen, with the tangential direction aligned with the axis of the dowel.

Two types of laminated bamboo board were used: bleached and caramelised. These differ in the commercial processing they have undergone, both of which treat sugars that would otherwise result in biodeterioration. The bleached bamboo strips are soaked in a bath of hydrogen peroxide solution at 70–80°C; the caramelised bamboo are treated with steam at 120–130°C [20].

For the timber specimens, Sitka spruce grown in Wales was used and graded as C16 according to EN 338 [21]. All timber specimens were cut from a solid section and no gluing was used. The ring structure of the timber was orientated so that the tangential

Table 1
Mean values of material tensile and shear properties (coefficient of variation is given in brackets when available).

Material	Tensile strength parallel to grain	Parallel to grain modulus	Tensile strength perp. to grain	Perp. to grain modulus	Shear modulus
	MPa	MPa	MPa	MPa	MPa
Bleached bamboo	124[a] (0.15)	–	3.14[a] (0.14)	–	–
Caramelised bamboo	90[a] (0.26)	8114[f] (0.10)	1.98[a] (0.13)	1208[f] (0.24)	945[c]
Sitka spruce C16 timber	67[b] (0.19)	8000[d]	2[e]	270[d]	500[d]

[a] [23].
[b] [24] (based on bending of small clear specimens, modulus of rupture).
[c] [25].
[d] [21].
[e] [26].
[f] [27].

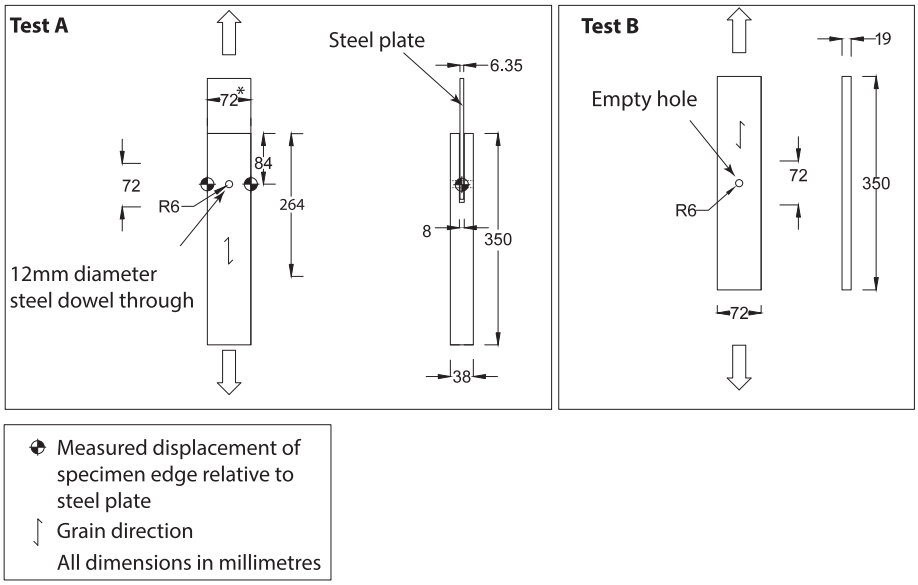

Fig. 1. Dowelled connection (left) and open-hole tension (right) test setups.

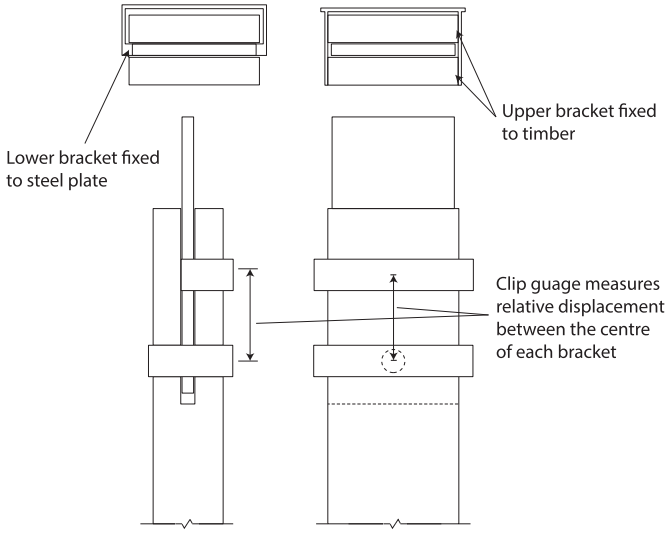

Fig. 2. Displacement measurement for Test A.

direction was in the plane of the specimen, with the radial direction along the axis of the dowel.

The moisture content of **and density of each** specimen was determined immediately after testing by **weighing and** oven drying according to BS EN 13183-1 [22]. Mean measured moisture contents were 7.0% for the bleached bamboo, 4.9% for the caramelised bamboo and 7.9% for the Sitka spruce.

Measured material properties in the literature for laminated bleached and caramelised Moso bamboo are summarised in Table 1, along with values for Sitka spruce timber.

Specimens were 72 mm wide, 38 mm thick and 350 mm long in the grain, or longitudinal, direction. The 38 mm thickness of bamboo was formed by two 19 mm-thick strips. A 12.3 mm hole was drilled 84 mm from the edge of each specimen, corresponding to the minimum edge distance recommended in timber design [2].

Additional direct tension tests were conducted on timber and bamboo plates with empty drilled holes to allow comparison of measured and modelled strain fields for a simple case. This specimen is shown as Test B in Fig. 1. These specimens were 72 mm wide, 19 mm thick and 350 mm long. A 12.3 mm hole was in the middle of each specimen, as shown in Fig. 1.

For all tests, a mechanical clip gauge was centred vertically on the edge of the specimens during testing. Tests were conducted using a 600 kN capacity universal test machine. Digital image correlation (DIC) was used in a number of tests to assess the two-dimensional strain fields on the surface of the specimens. For the DIC measurements, a high-contrast speckle pattern (white latex spray paint with photocopier toner broadcast on top) was applied to the specimen surface. A commercially available two-camera DIC system calculated strain fields from sequential images based on changes to the pattern resulting from deformation of the specimen.

4. Analytical program modelling

Both Test A and Test B were modelled using an orthotropic stress function for the stresses in the material around the hole. This form of stress function was derived by Lekhnitskii [28], and various researchers have used it to model the distribution of stress in an orthotropic plate loaded by a dowel, both in fibre-reinforced composites [29–32], and timber [33,34]. The method used to model the fields of stress and strain for Test A follows exactly the method developed by Hyer and Klang [30]. It models a hole in an infinite plate, which has been seen to give a reasonable approximation of the stresses around the hole when the breadth of the plate is greater than 2.5 times the diameter of the hole [33]. The minimum edge distance for timber design, used in this case, gives a breadth 6 times the diameter of the hole, so the infinite plate model was expected to be suitable.

The model is two dimensional, based on a state of plane stress. Boundary conditions are defined around the edge of the hole in three sections as shown in Fig. 3. The length of each section depends on the elastic properties of the bamboo or timber, and the coefficient of friction between the steel dowel and the bamboo or timber. In the ‘stick’ region, friction is not overcome, and the dowel and the surrounding material move together. In the ‘slip’ region, the dowel is in contact with the surrounding material, but friction is overcome, so the two materials slip relative to one another. The stick and slip regions therefore impose displacement boundary

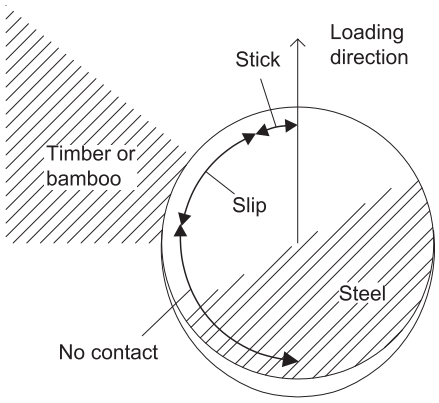

Fig. 3. Geometry for the orthotropic stress function model proposed by Hyer and Klang [30].

conditions on the timber or bamboo. In the 'no contact' region, there is no force transferred between the two materials.

The boundary conditions for Test B around the hole are that there is zero force on the surface of the hole, and that a uniform stress is applied to the plate far from the hole. The stress function for this geometry is more simple, and was given in the original work by Lekhnitskii [28].

5. Results and discussion

Fig. 4 shows the axial force-relative displacement diagrams for each test. The bamboo specimens exhibit a relatively sharp transition between the initially linear region and a lower-stiffness plastic region, while in the Sitka spruce, the transition is less well defined. The caramelised bamboo shows little or no plastic behaviour before fracture occurred. The ultimate failure of all specimens was by a crack, or a pair of cracks propagating from the dowel parallel to the loading direction.

Engineering design of dowelled connections in timber is based on the characteristic embedment strength of the timber. This value is given in design codes, based on testing of a large number of specimens of different species having different densities. The European design standard for timber, Eurocode 5 [2], uses the 5th percentile failure load as the characteristic load-carrying capacity, $F_{v,Rk}$, found using an empirical design rule based on the 5th percentile density, ρ (in kg/m^3):

$$F_{v,Rk} = 0.082(1 - 0.01d)\rho td \quad (1)$$

In which t is the width of the part and d is the diameter of the dowel, both in millimetres.

A similar prediction could therefore be made for the laminated bamboo using the same empirical equation – although the different molecular and cellular structure of bamboo may make that prediction inaccurate.

Eurocode 5 uses a representative moisture content of 12% at which the prescribed relationship between density and structural properties is considered valid. 12% is an approximate value of the equilibrium moisture content of a range of timber species at standard conditions of 20°C and 65% relative humidity. The 5th percentile density for the Sitka spruce was therefore adjusted to its estimated value at 12% moisture content.

Sharma et al. [23] reported the equilibrium moisture content of bleached and caramelised bamboo at these same standard conditions as being 8% for bleached, and 6% for caramelised. Table 2 shows the measured density of the specimens adjusted from their measured moisture contents to these representative moisture contents, and then adjusted to a common 12% moisture content for calculations according to Eurocode 5.

The results of these tests, shown in Fig. 5 and summarised in Table 3, gave an indication of the accuracy of such a prediction. The lower whisker of the left-hand box plot in Fig. 5 indicates the 5th percentile strengths determined from the present study.

The 5th percentile strength of the Sitka spruce, at 11.4 kN, exceeded the 9.3 kN predicted by the empirical design method in Eurocode 5, and in the bleached bamboo, the 5th percentile strength of 19.5 kN exceeded the 16.5 kN predicted for timber of the same density. The 5th percentile strength for the caramelised bamboo, 17.6 kN, was much closer to the predicted load, 16.1 kN, but, as shown in Fig. 4, the failure of the caramelised bamboo exhibited little plastic behaviour prior to fracture, thereby reducing the apparent failure load to a load near to the proportional limit. This lack of ductility makes plasticity-based design methods inappropriate.

The caramelised bamboo had the highest secant stiffness (~75 kN/mm), measured between 10% and 40% of the ultimate load after preloading to 40% of the ultimate load, following the method in EN 338 [21]. The bleached bamboo and the timber had similar stiffness to one another (~40 kN/mm). These values all significantly exceed the Eurocode 5 predicted stiffness, K_{ser}, based on material density as given by equation (2) [13], and shown in Table 3. This prediction might be expected to be inaccurate, since it takes no account of the geometry of the connection, except for the diameter of the dowel.

$$K_{ser} = \rho^{1.5} d/23 \quad (2)$$

Fig. 5 also shows a numerical comparison of the observed

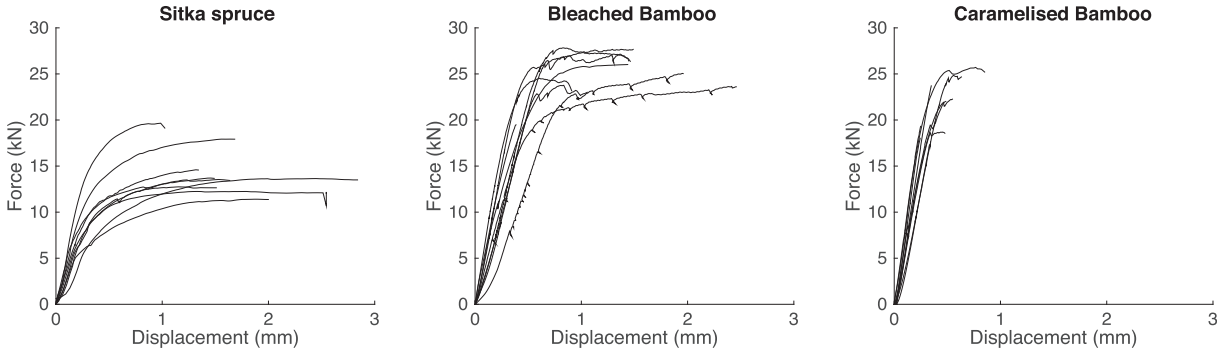

Fig. 4. Force–displacement plots for timber and bamboo specimens – fracture occurred at the end of each test.

Table 2
Connection capacity calculated using Eurocode 5 [2], using density adjusted to 12% moisture content (MC).

Material	Representative moisture content	5th Percentile density at representative MC	5th Percentile adjusted density at 12% MC	Embedment strength	Capacity
		kg/m^3	kg/m^3	N/mm^2	kN
Bleached bamboo	8%	636	660	48	17.1
Caramelised bamboo	6%	619	654	47	17.0
Sitka spruce	12%	357	357	26	9.3

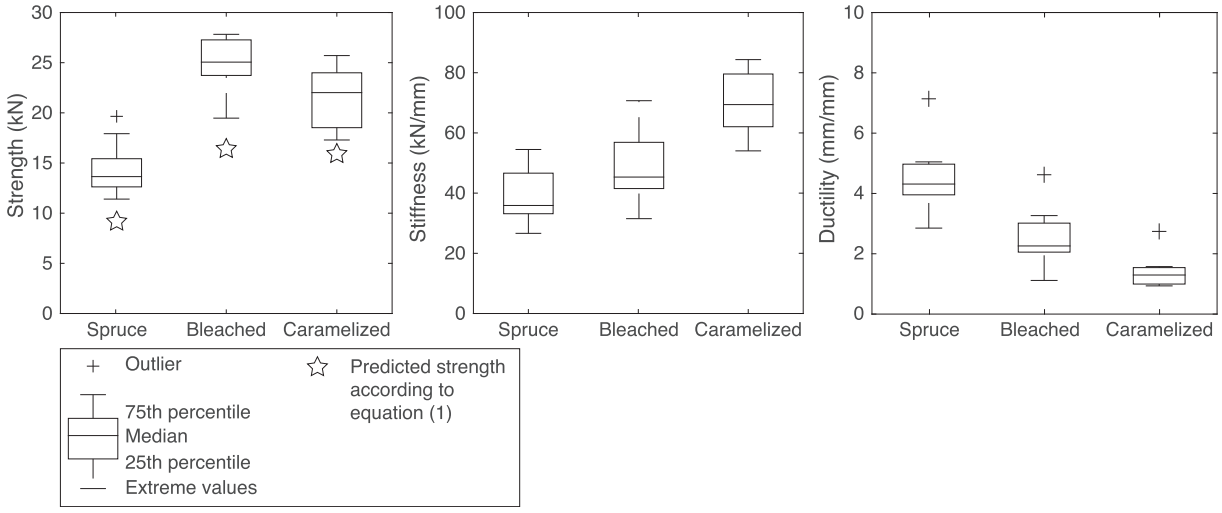

Fig. 5. Box plots for strength (left), stiffness (centre) and ductility (right) for three materials.

ductility expressed as the ratio of the ultimate slip and the slip at yield. The yield slip was determined as the intersection of the secant drawn between points at 10% and 40% of the ultimate load and the value of the ultimate load. The low ductility of the caramelised bamboo specimens can be seen. The Sitka spruce has a greater ductility than either bamboo, but the bleached bamboo has substantially higher ductility than the caramelised.

The failure mode of each specimen was assigned into one of four categories: (1) a single longitudinal splitting crack formed on the hole edge, within the middle third of the diameter drawn horizontally; (2) a pair of cracks forming a shear plug; (3) a single longitudinal crack forming outside the middle third; (4) or no visible crack. The three visible crack geometries are shown in Fig. 6.

Where a crack formed outside the middle third of the diameter, it is assumed that further loading would result in a shear plug being formed. For the purpose of analysis, therefore, the shear plug and the crack outside the middle third were considered together.

The orientation of the laminas of bamboo meant that the cracks caused by dowel loading would be in the radial-longitudinal (RL) plane for each of the laminates forming the sheet, as shown in Fig. 7.

Table 3
Comparison of measured properties with Eurocode 5 [2] predictions.

Material	5th Percentile strength		Mean stiffness	
	Eurocode 5	Measured	Eurocode 5	Measured
	kN	kN	kN/mm	kN/mm
Bleached bamboo	17.1	19.5	18.4	49.6
Caramelised bamboo	17.0	17.6	17.6	69.7
Sitka spruce timber	9.3	11.4	11.4	38.4

That is, the normal to the crack was in the radial direction, and the direction of crack growth in the longitudinal direction. The crack did not follow a glue line in any of the tests. In the timber, the crack formed preferentially in the tangential–longitudinal (TL) plane, often taking a slight angle in the specimen to follow this plane, as shown in Fig. 7.

The counts of the failure modes for each material are shown in Fig. 8. They show a clear distinction between laminated bamboo and Sitka spruce, with both types of processed bamboo generally failing by a shear plug or a crack outside the middle third, and the timber generally failing by a crack in the middle third. The latter was also seen as the dominant type of failure in a large number of tests on single-fastener connections in timber by Jorissen [11]. If the edge distance were sufficiently increased from 84 mm, the shear plug failure in the bamboo would transition to a single longitudinal crack as the shear resistance increases [35]. The edge distance of 84 mm is the minimum recommended in timber design guidance [2]. These results therefore show that design guidance for timber may not be directly applicable to laminated bamboo.

The resistance of the material to failure by a shear crack could be predicted using the shear capacity of the material measured by Sharma et al. [23]. The area of the failure surface was calculated for a single shear crack, as in the right hand image in Fig. 6, since it has been observed that failure can be initiated by a single shear crack. This type of failure could proceed to become a shear plug with two cracks under further loading. Table 4 shows the predicted failure loads. These loads must be considered as an upper bound estimate, since the stress concentration around the hole will mean that the failure stress in shear will be reached near the edge of the hole at a lower load. As a result, Table 4 shows that both types of bamboo failed at higher loads. The estimate of the failure load exceeds the

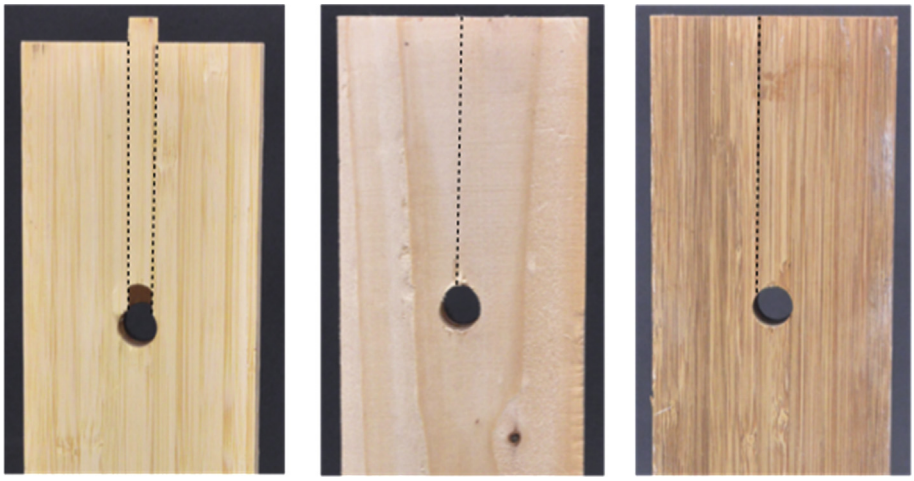

Fig. 6. Three observed fractures, with each crack shown by a dotted line: a shear plug in bleached bamboo (left), a crack in the central third of a Sitka spruce specimen (centre), and a crack in the outer third in caramelised bamboo (right).

capacity of all the Sitka spruce specimens shown in Fig. 5, which helps to explain why those specimens failed by other mechanisms.

A direct tensile test on a plate of caramelised bamboo with a central hole was used to validate the strain fields modelled using the orthotropic stress function. Fig. 9 shows the strain field measured using DIC, and the modelled strain field for this case. Two conclusions which may be drawn from these plots are that (1) the natural variation of the bamboo may lead to an asymmetrical distribution of strain, and that (2) the measured strains do not show the same sharp peaks and concentrations of strain as the model predicts. The two plots show generally the same shape of strain contour, giving confidence that an orthotropic elastic model of the material can give insight into its behaviour.

Fig. 7. Cracks in bleached bamboo (top) and Sitka spruce timber (bottom) – the crack in the bleached bamboo is typical in orientation for all bamboo specimens.

Fig. 10 shows the principal tension strain fields measured in each material during the tests. The colours (in the web version) show the maximum principal tension strain, and the black lines indicate the directions of those strains. In the Sitka spruce just one region of maximum principal strain is visible, spanning the centreline of the hole. The principal strain in this region is at close to 90° to the applied force, suggesting a tension perpendicular to the direction of the applied force. The crack due to these strains would be expected to form close to the centreline of the hole.

In the bleached bamboo, two separate peaks of maximum principal strain can be seen, and they cover an area where the direction of that strain is at approximately 45° to the applied force. This represents a shear force in the direction of the applied force, and therefore in the grain direction in the material. In the caramelised bamboo, two peaks in maximum principal strain may again be seen, perhaps closer to the centreline of the hole than in the bleached bamboo, but again with directions approximately 45° to the applied force.

To further analyse the behaviour of the dowelled connection, strain-field plots were generated from the complex stress function for an orthotropic material, as shown in Fig. 11. The mean material properties for C16 grade timber given in EN 338 [21] were used, along with a friction coefficient between steel and timber of 0.2, based on the measured values for spruce and pine [36]. Material properties for bamboo were taken from tests on caramelised Moso bamboo [27]. The friction coefficient between bamboo and steel was varied between the value for timber, and a higher value of 0.4

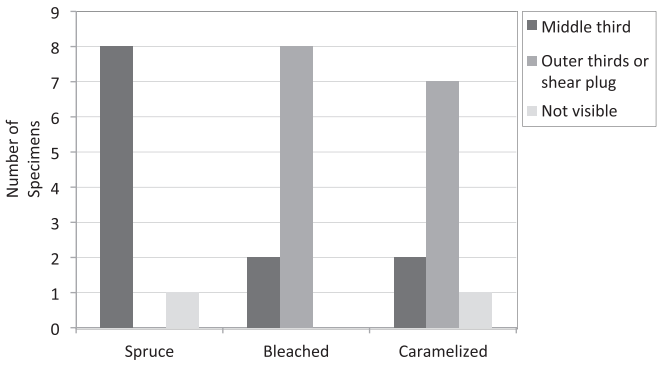

Fig. 8. Counts of failure modes by material.

Table 4
Predicted loads for failure by a single shear crack.

Material	Area of shear plane (78 mm × 30 mm)	Mean shear capacity [23]	Predicted specimen capacity	Mean observed capacity of specimens failing in this mode
	mm^2	N/mm^2	kN	kN
Bleached bamboo	2340	14	32.8	25.4
Caramelised bamboo	2340	16	37.4	21.6
Sitka spruce	2340	9	21.1	–

to investigate the change in the strain field with friction coefficient. The analysis aimed to identify the properties that lead to the two peaks of maximum strain seen in the bamboo in Fig. 10, in contrast to the single peak in the timber.

The modelled strain field in the Sitka spruce, on the left in Fig. 11, shows that there are, in fact, two peaks in maximum principal strain using typical properties for timber. In that model, however, the peaks are close together, and merge not far from the edge of the hole. In the middle plot, it can be seen that two distinct regions of maximum principal shear stress occur for bamboo; this is due to the low shear modulus in comparison to the elastic modulus in the horizontal (perpendicular to grain) direction. This results in the shear deformation being larger than the tensile deformation perpendicular to grain. These two peaks become further separated as the friction coefficient is increased from 0.2 to 0.4 in the right hand plot in Fig. 11. This latter behaviour shows a closer qualitative resemblance to the measured strain fields for bamboo.

The strain field around the bamboo is qualitatively different to that in the Sitka spruce. This is due to the different orthotropic material properties of the bamboo, particularly the fact that the shear modulus is lower than the perpendicular to grain modulus in bamboo, while the opposite is true in Sitka spruce. The difference in the strain field may also be due in part to a higher friction coefficient between steel and bamboo than between steel and timber, though this has not been directly tested either in this study or elsewhere. The models suggest that the shear properties of the material and the friction coefficient are key to the performance of the connection.

6. Conclusion

This experimental study has highlighted the difference in embedment and fracture behaviour of dowelled connections in Sitka spruce and laminated bamboo, and has shown that there are substantial differences in the same properties between bamboo treated by bleaching and caramelisation. In Sitka spruce, failure is generally by formation of a crack at the location of maximum tensile stress perpendicular to the grain. In contrast, fracture in laminated bamboo tends to be by formation of cracks at the locations of maximum shear stress, and failure may be by a single one of these cracks or by a shear plug. This tendency towards a different failure mechanism indicates that design rules and practices used to prevent splitting in timber construction are not directly applicable to laminated bamboo.

Caramelised bamboo exhibits brittle behaviour in comparison with both bleached bamboo and Sitka spruce. In a complete connection, this may mean that splitting occurs before plastic hinges are allowed to form in the dowel. These hinges are vital to the method used to predict the ultimate load in timber connections, and therefore the same method should not be directly transposed to engineering connections in laminated bamboo.

Additionally, full-field strain measurements suggest that shear deformation is a more substantial component of the deformation in bamboo connections than in timber. This corresponds to the observation that cracks in bamboo initiated at points of maximum shear stress, where in the Sikta spruce specimens cracks initiated due to tension perpendicular to the grain. Timber engineering design rules specify minimum edge distances to prevent this form

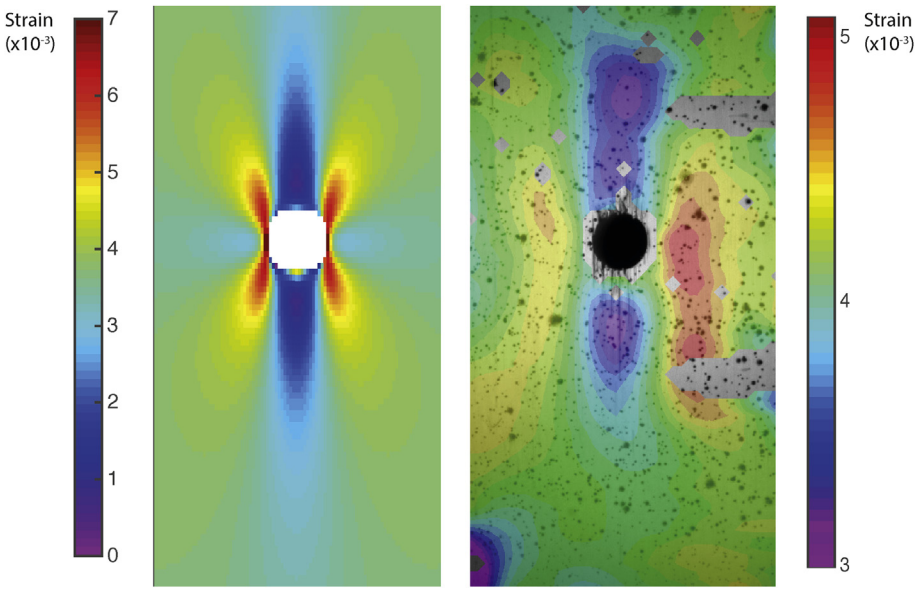

Fig. 9. Qualitative comparison of modelled and measured strain fields in the caramelised bamboo plate with hole – the plots show strain in the vertical direction. (Please refer to the web version for colours)

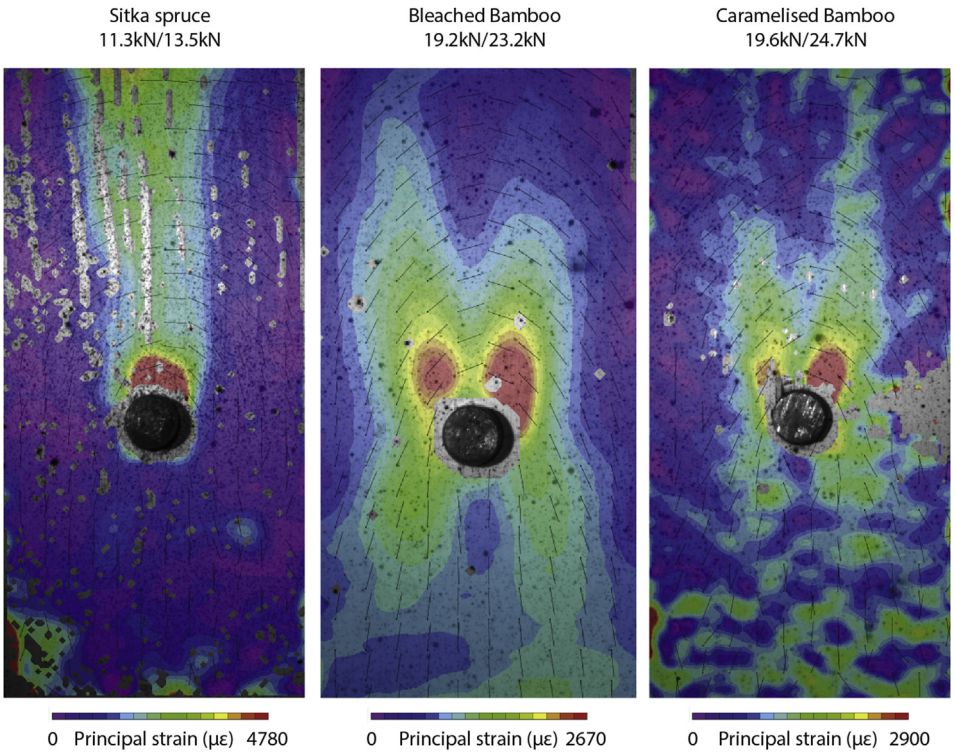

Fig. 10. Maximum principal tension strains in the three materials – loads stated are force for strain field shown/force at failure – black lines indicate directions of principal tension strain. (Please refer to the web version for colour images)

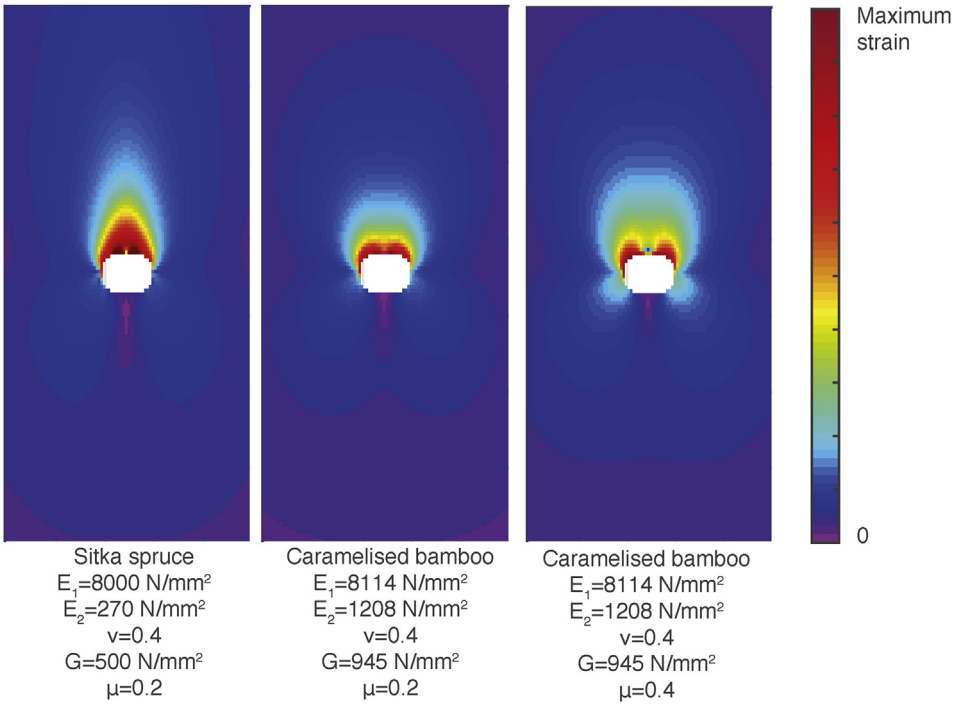

Fig. 11. Fields of maximum principal strain, modelled using a complex stress function, for C16 timber according to EN 338 [21], and laminated Moso bamboo using elastic moduli measured from Yang et al. (2010). (Please refer to the web version for colour images)

of failure, and those rules will have to be adapted or changed before being applied to design of bamboo.

To enable reliable design of dowelled connections in laminated bamboo, research is needed to better understand the failure mechanisms in embedment. The different preservative treatments applied to the bamboo affected the ductility before fracture, and research is required to understand how these and other chemical processes affect the load resistance and fracture of bamboo.

It has been shown that the behaviour of laminated bamboo in embedment has several qualitative differences to that in timber,

which must be taken into account in the development of design equations and standards. Rules developed for the design of timber structures may not be directly applied to laminated bamboo.

Acknowledgements

The presented work is supported by a Leverhulme Trust Programme Grant, and EPSRC Grant EP/K023403/1. Tests were conducted in the University of Pittsburgh Watkins–Haggart Structural Engineering Laboratory. The authors would also like to thank Charles Hager, Tianqiao Liu, Shawn Platt, Michael Sweriduk, Janine Domingos Vieira, and Elizabeth Crumley.

References

[1] Johansen KW. Theory of timber connections. IABSE Publ 1949;9:249–62.
[2] BSI. Eurocode 5 design of timber structures. BSI; 2009.
[3] Whale LRJ, Smith I, Larsen HJ. Design of nailed and bolted joints. In: Meeting of CIB working Group 18 on timber structures, Dublin; 1987.
[4] Sjödin J, Enquist B, Serrano E. Contact-free measurements and numerical analyses of the strain distribution in the joint area of steel-to-timber dowel joints. Holz Als Roh-Und Werkst 2006;64:497–506. http://dx.doi.org/10.1007/s00107-006-0112-1.
[5] Sjödin J, Serrano E, Enquist B. An experimental and numerical study of the effect of friction in single dowel joints. Holz Als Roh-Und Werkst 2008;66:363–72. http://dx.doi.org/10.1007/s00107-008-0267-z.
[6] Foust BE, Lesniak JR, Rowlands RE. Stress analysis of a pinned wood joint by grey-field photoelasticity. Compos Part B Eng 2014;61:291–9. http://dx.doi.org/10.1016/j.compositesb.2014.01.041.
[7] Rodd PD, Leijten AJM. High-performance dowel-type joints for timber structures. Prog Struct Eng Mater 2003;5:77–89. http://dx.doi.org/10.1002/pse.144.
[8] Egan B, McCarthy CT, McCarthy MA, Frizzell RM. Stress analysis of single-bolt, single-lap, countersunk composite joints with variable bolt-hole clearance. Compos Struct 2012;94:1038–51.
[9] Olmedo Á, Santiuste C. On the prediction of bolted single-lap composite joints. Compos Struct 2012;94:2110–7. http://dx.doi.org/10.1016/j.compstruct.2012.01.016.
[10] Chang F-K, Chang K-Y. A Progressive damage model for laminated composites containing stress concentrations. J Compos Mater 1987;21:834–55. http://dx.doi.org/10.1177/002199838702100904.
[11] Jorissen AJM. Double shear timber connections with dowel type fasteners. Heron 1999;44:131–61.
[12] Dorn M, de Borst K, Eberhardsteiner J. Experiments on dowel-type timber connections. Eng Struct 2013;47:67–80. http://dx.doi.org/10.1016/j.engstruct.2012.09.010.
[13] BSI. Timber structures. Test methods. Cyclic testing of joints made with mechanical fasteners. BSI; 2001.
[14] Ashby MF, Easterling KE, Harrysson R, Maiti SK. The fracture and toughness of woods. Proc R Soc A Math Phys Eng Sci 1985;398:261–80.
[15] Stanzl-Tschegg SE, Navi P. Fracture behaviour of wood and its composites. A review COST Action E35 2004–2008: wood machining – micromechanics and fracture. Hfsg 2009;63:139–49. http://dx.doi.org/10.1515/HF.2009.012.
[16] Mitch D, Harries KA, Sharma B. Characterization of splitting behavior of bamboo culms. J Mater. Civ Eng 2010;22:1195–9. http://dx.doi.org/10.1061/(ASCE)MT.1943-5533.0000120.
[17] Amada S, Untao S. Fracture properties of bamboo. Compos Part B Eng 2001;32:451–9. http://dx.doi.org/10.1016/S1359-8368(01)00022-1.
[18] Habibi MK, Lu Y. Crack propagation in bamboo's hierarchical cellular structure. Sci Rep 2014;4. http://dx.doi.org/10.1038/srep05598.
[19] BSI. Timber structures. Test methods. Determination of embedment strength and foundation values for dowel type fasteners. BSI; 2007.
[20] van der Lugt P. Design interventions for stimulating bamboo commercialization: Dutch design meets bamboo as a replicable model. Delft, Netherlands: VSSD; 2008.
[21] BSI. Structural timber. Strength classes. BSI; 2009.
[22] BSI. Moisture content of a piece of Sawn timber. BSI; 2002.
[23] Sharma B, Gatoo A, Ramage MH. Effect of processing methods on the mechanical properties of engineered bamboo. Constr Build Mater 2015;83:95–101. http://dx.doi.org/10.1016/j.conbuildmat.2015.02.048.
[24] Lavers GM. The strength properties of timber. BRE; 1983.
[25] Aschheim M, Gil-Martín LM, Hernández-Montes E. Engineered bamboo I-Joists. J Struct Eng-Asce 2010;136:1619–24. http://dx.doi.org/10.1061/(ASCE)ST.1943-541X.0000235.
[26] Hull D, Clyne TW. Introduction to composite materials. Cambridge University Press; 1996.
[27] Sharma B, Ramage MH. EN 408 testing of Moso outdoor laminated bamboo. Prepared for Moso International BV. Cambridge, United Kingdom: University of Cambridge; 2015. p. 96.
[28] Lekhnitskii SG. Anisotropic plates. 2nd ed. New York: Gordon and Breach; 1968.
[29] Zhang K-D, Ueng CES. Stresses around a pin-loaded hole in orthotropic plates. J Compos Mater 1984;18:432–46. http://dx.doi.org/10.1177/002199838401800503.
[30] M.W. Hyer, E.C. Klang, Contact stresses in pin-loaded orthotropic plates. 1985; 21: 957–975.
[31] Aluko O, Whitworth HA. Analysis of stress distribution around pin loaded holes in orthotropic plates. Compos Struct 2008;86:308–13. http://dx.doi.org/10.1016/j.compstruct.2008.06.001.
[32] Derdas C, Kostopoulos V. On the bearing failure of laminated composite pin-loaded joints: exploitation of semi-analytical solutions for the determination of the stress state. Strain 2011;47:320–32. http://dx.doi.org/10.1111/j.1475-1305.2010.00772.x.
[33] Echavarría C, Haller P, Salenikovich A. Analytical study of a pin–loaded hole in elastic orthotropic plates. Compos Struct 2007;79:107–12. http://dx.doi.org/10.1016/j.compstruct.2005.11.038.
[34] Reynolds T, Harris R, Chang W-S. An analytical model for embedment stiffness of a dowel in timber under cyclic Load, vol. 71; 2013. p. 609–22. http://dx.doi.org/10.1007/s00107-013-0716-1.
[35] Platt S, Harries KA. In: Strength of bolted bamboo laminate connections. Winnipeg, Canada: NOCMAT; 2015.
[36] McKenzie WM, Karpovich H. The frictional behaviour of wood. Wood Sci Technol 1968;2:139–52. http://dx.doi.org/10.1007/bf00394962.